

Quasiparticles, coherence and nonlinearity: exact simulations of RF-spectroscopy of strongly interacting one-dimensional Fermi gases

M.J. Leskinen¹, V. Apaja², J. Kajala¹, P. Törmä^{1*},

¹*Department of Engineering Physics, P.O.Box 5100,
02015 Helsinki University of Technology, Finland*

²*Department of Physics, Nanoscience Center,
P.O.Box 35, 00014 University of Jyväskylä, Finland**

Abstract

The excitation spectrum of a quantum state can be measured by outcoupling particles and creating quasiparticles. In ultracold Fermi gases, RF-spectroscopy [1, 2, 3, 4, 5, 6, 7] realizes such outcoupling. One of the two interacting (pseudo)spin components is coupled by an RF field to a third component. This can be viewed as a quasiparticle creation process [8, 9, 10, 11, 12, 13, 14, 15, 16, 17] analogous to tunneling. It can also be viewed as a coherent rotation in (pseudo)spin space [18, 19, 20, 21], analogous to NMR experiments in superfluid ³He [22, 23, 24]. The picture which applies depends on the coherence of the time evolution [21]. We suggest here that RF-spectroscopy in ultracold gases provides an interesting crossover between these descriptions that could be used for studying decoherence in quantum measurement. We compare the coherent rotation and quasiparticle descriptions, and study nonlinear effects, by exact simulations of the many-body state and the dynamics in one dimension. Deviations from the linear response are found to suppress the pairing contribution to the RF line shifts in the coherent case.

*Electronic address: paivi.torma@hut.fi

The system considered is described by the Hamiltonian

$$\begin{aligned}
H = & \sum_{\sigma=1,2,f} \int d\mathbf{r} \Psi_{\sigma}^{\dagger}(\mathbf{r}) \left[-\frac{\nabla^2}{2m} - \mu_{\sigma} \right] \Psi_{\sigma}(\mathbf{r}) + U_{12} \int d\mathbf{r} \Psi_1^{\dagger}(\mathbf{r}) \Psi_2^{\dagger}(\mathbf{r}) \Psi_2(\mathbf{r}) \Psi_1(\mathbf{r}) + \\
& U_{1f} \int d\mathbf{r} \Psi_1^{\dagger}(\mathbf{r}) \Psi_f^{\dagger}(\mathbf{r}) \Psi_f(\mathbf{r}) \Psi_1(\mathbf{r}) + \Omega \int d\mathbf{r} \Psi_f^{\dagger}(\mathbf{r}) \Psi_2(\mathbf{r}) + \Omega \int d\mathbf{r} \Psi_2^{\dagger}(\mathbf{r}) \Psi_f(\mathbf{r}) + \\
& \frac{\delta}{2} \int d\mathbf{r} [\Psi_2^{\dagger}(\mathbf{r}) \Psi_2(\mathbf{r}) - \Psi_f^{\dagger}(\mathbf{r}) \Psi_f(\mathbf{r})], \tag{1}
\end{aligned}$$

where U_{12} and U_{1f} are the interaction strengths, $\mu_1 = \mu_2 \equiv \mu$ the chemical potentials, m is the mass, and Ω the field (effective) Rabi frequency. For a non-interacting system ($U_{12} = U_{1f} = 0$), the spectrum of transferring particles to the (initially empty) final state f has a peak at frequency ω_{free} . For an interacting system, the maximum transfer of atoms from state 2 to state f takes place at a certain RF frequency ω_{RF} that may be different from ω_{free} by some detuning $\delta = \omega_{RF} - \omega_{free}$.

In the quasiparticle picture, assuming BCS state with excitation energy E_k , gap Δ and linear response for the field, the detuning is bound by the energy conservation relation [8]

$$\delta = E_k + \epsilon_k - \mu = \sqrt{(\epsilon_k - \mu)^2 + \Delta^2} + \epsilon_k - \mu \tag{2}$$

which gives the threshold detuning (minimum δ_{th} is obtained for $\epsilon_k = 0$)

$$\delta_{th} = \sqrt{\mu^2 + \Delta^2} - \mu \simeq \frac{\Delta^2}{2\mu} \simeq \frac{\Delta^2}{2E_F}. \tag{3}$$

Including the Hartree interactions gives

$$\begin{aligned}
\delta_{th} = & \sqrt{(-\mu + U_{12}n_1)^2 + \Delta^2} - \mu + U_{1f}n_1 \simeq (U_{1f} - U_{12})n_1 + \frac{\Delta^2}{2(\mu - U_{12}n_1)} \\
& \simeq (U_{1f} - U_{12})n_1 + \frac{\Delta^2}{2E_F}, \tag{4}
\end{aligned}$$

where E_F is the Fermi energy and n_{σ} denotes the densities for different components. The threshold δ_{th} corresponds well to the maximum peak position, because the spectral weight is suppressed below the threshold. Eq.(3) gives also the molecular binding energy $\delta_{th} \sim 2|\mu|$, for $\mu < 0$ and $|\mu| \gg \Delta$.

In the coherent rotation picture, within the linear response, the mean value for the frequency shift, $\bar{\delta}$, can be obtained from the sum rules [19, 20]

$$\bar{\delta} = \frac{\int d\delta \delta \chi''(\delta)}{\int d\delta \chi''(\delta)} = (U_{1f} - U_{12}) \frac{\langle \int d\mathbf{r} \Psi_1^{\dagger}(\mathbf{r}) \Psi_2^{\dagger}(\mathbf{r}) \Psi_2(\mathbf{r}) \Psi_1(\mathbf{r}) \rangle}{n_2} \tag{5}$$

which in the BCS limit becomes [19]

$$\bar{\delta} = (U_{1f} - U_{12})n_1 + (U_{1f} - U_{12})\frac{\Delta^2}{U_{12}^2 n_2}. \quad (6)$$

The Hartree term $(U_{1f} - U_{12})n_1$ is the same in Eq.(4) and in Eq.(6). Neglecting it one obtains for $U_{1f} = 0$ that

$$\delta_{th} \simeq \frac{\Delta^2}{2E_F} \quad (7)$$

and

$$\bar{\delta} = \frac{\Delta^2}{U_{12}n_2}. \quad (8)$$

Both the quasiparticle and coherent rotation pictures predict that the frequency shift is proportional to Δ^2 , but for different reasons. For the coherent rotation, the term $\frac{\Delta^2}{U_{12}}$ is the difference between the total energy of the final and initial many-body states, and dividing it by n_2 gives the energy difference per particle. In the quasiparticle picture, the suppression of pairing by the Fermi energy, $\delta_{th} \simeq \frac{\Delta^2}{E_F}$, appears because the particles that can be excited with the smallest energy are at the bottom of the Fermi sea ($\epsilon_k = 0$). Note that in some other contexts (e.g. tunneling in metals), the states at the bottom of the Fermi sea are Pauli blocked, whereas here the final state is initially empty. In fact, by having some initial occupation of the final state, the dependence of δ_{th} on Δ could be brought towards $\delta_{th} \sim \Delta$ [8, 9, 25] in the quasiparticle picture, whereas in the coherent rotation picture the Δ^2 dependence would be unchanged. For the coherent rotation, the term $(U_{12} - U_{1f})$ multiplying Δ^2 leads to the zero shift $\bar{\delta} = 0$ if the interaction strengths are the same, i.e. the interaction is SU(2) invariant in spin space [24]. In contrast, in the simplest quasiparticle picture (Eq.(4)) the term proportional to Δ^2 does not depend on the final state interactions. This can be valid for many-body pairing with weak interactions: a single outcoupled particle does not form a Cooper pair because there is no Fermi sea for the particles in the final state. For strong interactions and/or if bound states exists, pairing can take place without the Fermi sea. Such a 1-f bound state can be added to the quasiparticle picture to describe bound-bound transitions [12, 17].

The shape of the spectra in the coherent rotation and quasiparticle pictures allows distinguishing between them in the experiment. In the quasiparticle picture, the spectral peak is asymmetric with a long tail. In the coherent rotation description, the spectra are symmetric and not broadened by interactions [19, 21]. We will now compare the coherent and quasiparticle pictures in a one-dimensional system, paying particular attention to the validity of the

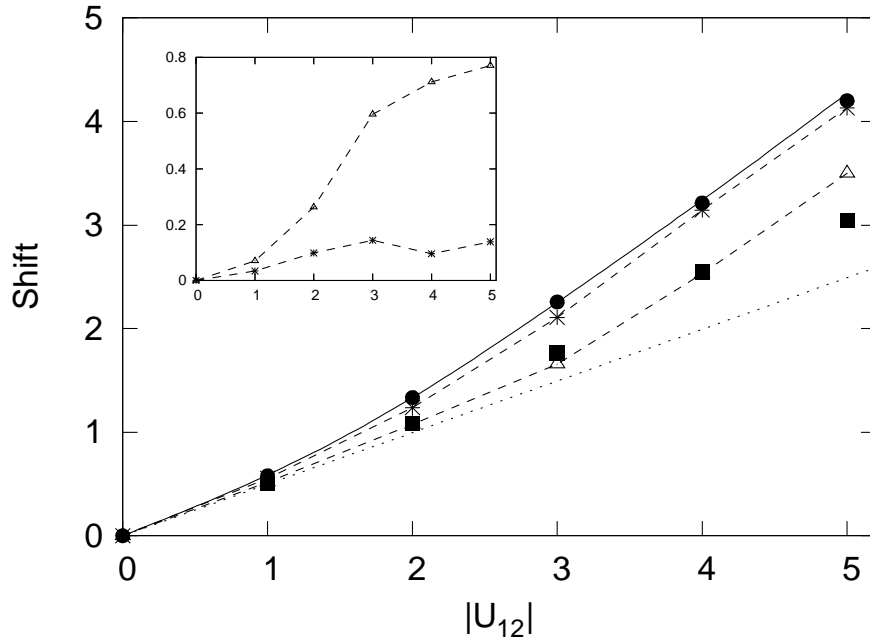


Figure 1: The frequency shifts for different interaction strengths $U_{12} \leq 0$. The circles represent 1.0%, stars 10% and triangles 50% particle transfer. The linear response - sum rule result (solid line) works well for weak interactions or if the amount of transferred particles is small. The result given by Fermi golden rule (squares) and Hartree term $U_{12}n_1$ (dotted line) are presented. In the inset the difference between the sum rule and numerical results are presented.

linear response. All the previous works in the literature on RF-spectroscopy have assumed linear response (only in [26] an approximative non-linear model was considered). We thus present the first results with no approximations (linear or higher order) in the field-matter interaction.

We consider the Hamiltonian (1) within the one-dimensional, one-band Hubbard model with nearest neighbour hopping and on-site interaction (see Methods). After calculating the ground state within the matrix product state (MPS) formalism [27], we simulate the dynamics by applying a square pulse. For each detuning, we calculate the expectation value for the number of atoms in the final state after the pulse and thus obtain the spectrum. The numerically obtained RF line shift is denoted as δ_{num} .

Figure 1 shows the shift δ_{num} as a function of the interaction strength, U_{12} , when $U_{1f} = 0$. In Figure 2, we vary $U_{1f} \neq 0$ and keep U_{12} fixed. For comparison, we show the shift of the peak $\bar{\delta}$ as given by the sum rule within the linear response theory, Eq. (5), where we calculate $\langle \int d\mathbf{r} \Psi_1^\dagger(\mathbf{r}) \Psi_2^\dagger(\mathbf{r}) \Psi_2(\mathbf{r}) \Psi_1(\mathbf{r}) \rangle$ from the numerical results. Having the BCS result (6) in mind,

we also plot the Hartree mean field contribution $U_{12}n_1$, and extract the quantity Δ from (5) and (6) (see Methods). Using Δ obtained in this way we use the standard BCS description to present results given by the quasiparticle picture.

As Figure 1 shows, the numerical result deviates from the linear response sum rule result (Eq. (5)) by an increasing amount for increasing interactions, if the number of particles transferred is e.g. 50 %, or even 10 % of the particle number in state 2 (i.e. 25 % / 5 % of the total particle number). Only when as little as ~ 1 % of the atoms are transferred, the linear response is strictly valid. For $U_{12} > 0$, the deviation is found to be similar. Figure 2 shows the effect of nonzero U_{1f} , i.e. the simple amplification by the factor $(U_{1f} - U_{12})$ in Eq.(5). As expected for a coherent process, the spectra are symmetric and the width depends only on Ω as can be seen in Figure 3. We checked whether the simulated time evolution corresponds to simple Rabi oscillations with some effective detuning caused by interactions: we fitted to the numerical oscillations the maximum peak height $\frac{4\Omega^2}{\delta'^2 + 4\Omega^2}$ and the period $2\pi(\delta'^2 + 4\Omega^2)^{-1/2}$ with δ' as the fitting parameter. The fitting was found to fail hand in hand with the failure of linear response approximation for increasing interactions. This is in accordance with the observation (see Figure 1) that nonlinear effects show up when the pairing contribution starts to become considerable compared to the Hartree term (for Hartree shifts alone, the simple Rabi picture should be valid). For 50 % of transferred particles, the suppression of the remaining pairing contribution by nonlinearity ranges from 30 % to 100 % for the values used in Figure 1. In the simplest quasiparticle picture, the nonlinear shift may not necessarily be this dramatic since higher order processes might produce primarily subthreshold weight rather than shift of the peak. However, our results show that one should be cautious with the linear response approximation in any type of RF spectroscopy measurement, whenever pairing is measured.

It is now interesting to compare the coherent and quasiparticle pictures from the point of view of a quantum measurement. In the former, the system decoheres only after the pulse. In the latter, the measurement instantaneously projects the system into the total final state which can be e.g. one free particle in state f and one quasiparticle in the superfluid. The starting point for both descriptions (within the linear response) is the imaginary part of the correlation function $-i \int d\mathbf{r} \langle T[\psi_2^\dagger(\mathbf{r}, t)\psi_f(\mathbf{r}, t)\psi_f^\dagger(0, 0)\psi_2(0, 0)] \rangle$ which, as well as the sum rules, corresponds to the coherent Hamiltonian evolution. On the other hand, Fermi golden rule corresponds to the instantaneous projection (Fermi golden rule result is often

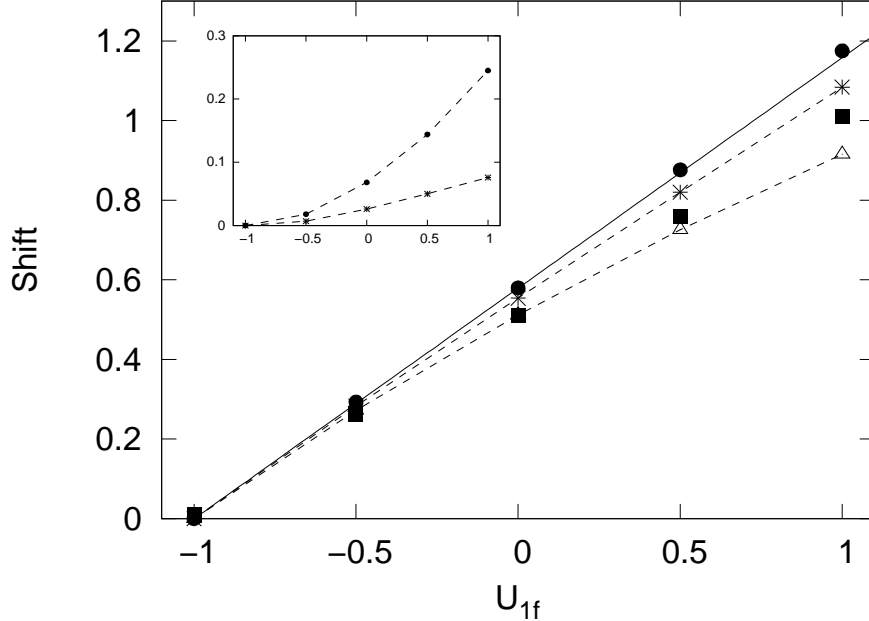


Figure 2: The frequency shifts for different final state interaction strengths U_{1f} ($U_{12} = -1.0$). The circles represent 1.0 %, stars 10 % and triangles 50 % particle transfer. The sum rule is shown in solid line. In the inset the difference between sum rule and numerical results are presented.

obtained in an experiment for a long, weak excitation but formally it describes an instantaneous projection). Fermi golden rule follows from $-i \int d\mathbf{r} \langle T[\psi_2^\dagger(\mathbf{r}, t)\psi_f(\mathbf{r}, t)\psi_f^\dagger(0, 0)\psi_2(0, 0)] \rangle$ by dividing this expression to the final and initial state contributions. The measurement done is thus defined by the way the correlation function is calculated. It is possible to calculate $-i \int d\mathbf{r} \langle T[\psi_2^\dagger(\mathbf{r}, t)\psi_f(\mathbf{r}, t)\psi_f^\dagger(0, 0)\psi_2(0, 0)] \rangle$ by including final state interactions in a fully self-consistent way [19], corresponding to coherent rotation of all particles. The simplest quasiparticle picture (Eq.(4)) is obtained by a straightforward factorization of the correlation function. Then the spectrum obtained no longer satisfies the f-sum rule, i.e. it does not describe coherent evolution but a projection measurement to the chosen final state. If the final state is likely to have bound states or strong interactions, they should be included in the quasiparticle description [15, 17].

Some of the spectra obtained in the early RF experiments on pairing [3, 5, 6] are symmetric although this could be partly due to broadening by inhomogeneous density in [3, 5]. In any case, the spectral shapes depend on the interaction strength, density and temperature, and the quasiparticle picture can be applied to describe qualitative features such as the double peak structure [11, 13, 16]. Exact modelling of the intermediate cases between the

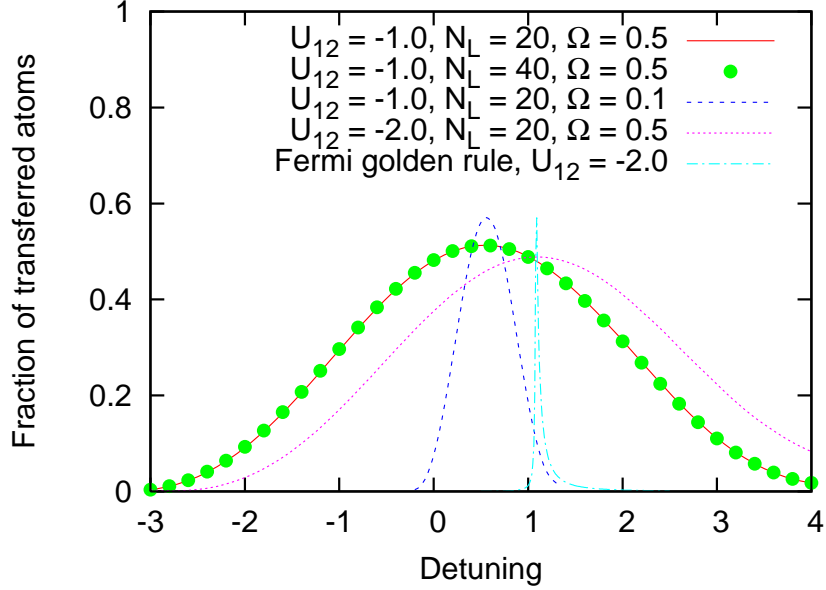


Figure 3: Spectra for different values of coupling Ω , interaction U_{12} and the number of lattice sites N_L . The shape of Fermi golden rule result is shown (in arbitrary units). The width of the spectrum depends only on the coupling Ω . The duration of the pulse is $0.8\Omega^{-1}$.

coherent and simple quasiparticle pictures - or realizing the experiment in such a way that one picture is strictly valid - becomes crucial in high precision measurements of the pairing gap. The recently obtained spectra [7] in the case where final state interactions have been reduced show clearly asymmetric shape.

For strong initial state and weak final state interactions the eigenstate wavefunctions of the initial and final states are very different: the RF field then couples one state to a continuum of states. Decoherence is the strongest when a state is coupled to a large number of other states, which enforces a projection measurement. This is obviously the case for the molecule continuum dissociation process. If the final state resembles the initial state, the process is more likely to stay coherent. This can happen e.g. for stronger final state interactions. The extreme case is the Hartree mean fields which do not affect the wave function in a homogeneous system; fully coherent rotation was observed in measurements of the Hartree shifts [2, 18]. The experimental observation of both quasiparticle and coherent rotation type results for ultracold Fermi gases, and the possibility of a tunable crossover between them suggest that RF spectroscopy in these systems may be suited for studying the long standing problem of quantum measurement and the question of how decoherence

sets in in the measurement process, in the context of many-body states.

In summary, we have compared the exact coherent dynamics of RF spectroscopy of interacting Fermions in one dimension to the quasiparticle picture within the BCS formalism. We have also pointed out a potential connection with quantum measurement and decoherence. Large suppression of the pairing shift from the linear response prediction was found when the transferred particle numbers were more than $\sim 1\%$. Although the precise numbers are for the case studied (1 D, coherent rotation), it is possible that some of the pairing related RF line shifts observed experimentally have been suppressed by nonlinearity. In the future, it would be especially interesting to consider 1 D systems where exact theory and modeling is possible, to understand both coherent and incoherent processes in RF spectroscopy. The deviations from linear response for strong interactions found here also indicate that such systems could display other interesting nonlinear phenomena in the field-matter interaction.

METHODS

The Hamiltonian (1) reduces to the Hubbard hamiltonian when the single band lattice model is assumed within the tight binding approximation:

$$\begin{aligned}
 H = & -J \sum_{\langle ij \rangle \sigma} c_{i\sigma}^\dagger c_{j\sigma} + U_{12} \sum_i c_{i1}^\dagger c_{i2}^\dagger c_{i2} c_{i1} + U_{1f} \sum_i c_{i1}^\dagger c_{if}^\dagger c_{if} c_{i1} + \sum_{i\sigma} \mu_\sigma c_{i\sigma}^\dagger c_{i\sigma} \\
 & + \sum_i \frac{\delta}{2} \left(c_{i2}^\dagger c_{i2} - c_{if}^\dagger c_{if} \right) + \Omega \sum_i \left(c_{if}^\dagger c_{i2} + c_{i2}^\dagger c_{if} \right),
 \end{aligned} \tag{9}$$

where $c_{i\sigma}^\dagger$ creates a particle σ to site i .

Note that no renormalization is needed for the interaction strengths due to the natural cutoff by the first band. The 2f interactions are neglected. We set $J = 1$ in all calculations, all other quantities are then in units of J . The relation between J , U and the parameters for atoms in an optical lattice are as in [28]. The chemical potentials are chosen so that the density becomes corresponding to the half filling. The final state is initially empty.

For calculating the ground state and for simulating the dynamics we use the matrix state product method as described in [27, 29]. This formalism is especially suited for simulating time evolution in sufficiently regular systems. The ground state (when $\Omega = \delta = 0$) is obtained by operating to the initial state with imaginary time evolution operator which we approximate by the Forest-Ruth formula [30]. After finding the ground state we operate in real time to calculate the time-evolution of the state.

The errors due to the numerical method are controlled and very small: we have varied

the size of the matrices in the matrix product state (which basically controls the truncation of the Hilbert space needed for a computationally feasible calculation) from 5 to 12, and the results start to converge around 5 (depending on the interaction), and the error still left in the results fits within the data point symbols used for plotting the results. The simulations are double-checked using two different computer codes (one in C++, the other in Fortran) written independently by two persons, which should eliminate the possibility of trivial mistakes in the numerics.

In our calculations the gap Δ of the BCS-theory was substituted into Fermi golden rule. We evaluated the gap from the on-site correlation $U\langle c_{i1}^\dagger c_{i2}^\dagger c_{i2} c_{i1} \rangle \approx U n_1 n_2 + \Delta^2 U^{-1}$. This correlation can be calculated from the ground state of the system.

The results shown here are for densities close to the half filling. We have also done simulations for low densities which correspond to the continuum 1D case, and found that the results are essentially the same. In calculations we have mainly used 20 lattice sites but also bigger lattices have been tested. The tests gave similar results as shown in Figure 3.

Acknowledgments

This work was supported by the National Graduate School in Materials Physics, Academy of Finland (Projects Nos. 115020, 213362, 121157) and conducted as a part of a EURYI scheme award. See www.esf.org/euryi.

-
- [1] C. A. Regal and D. S. Jin, Phys. Rev. Lett. **90**, 230404 (2004).
 - [2] S. Gupta, Z. Hadzibabic, M.W.Zwierlein, C. Stan, K. Dieckmann, C. Schunck, E. van Kempen, B. Verhaar, and W. Ketterle, Science **300**, 1723 (2003).
 - [3] C. Chin, M. Bartenstein, A. Altmeyer, S. Riedl, S. Jochim, J. H. Denschlag, and R. Grimm, Science **305**, 1128 (2004).
 - [4] M. Bartenstein, A. Altmeyer, S. Riedl, R. Geursen, S. Jochim, C. Chin, J. H. Denschlag, R. Grimm, A. Simoni, E. Tiesinga, et al., Phys. Rev. Lett. **94**, 103201 (2005).
 - [5] C. H. Schunck, Y. Shin, A. Schirotzek, M. W. Zwierlein, and W. Ketterle, Science **316**, 867 (2007).

- [6] Y. Shin, C. H. Schunck, A. Schirotzek, and W. Ketterle, Phys. Rev. Lett. **99**, 090403 (2007).
- [7] C. H. Schunck, Y. Shin, A. Schirotzek, and W. Ketterle (2008), arXiv:0802.0341.
- [8] P. Törmä and P. Zoller, Phys. Rev. Lett. **85**, 487 (2000).
- [9] G. M. Bruun, P. Törmä, M. Rodriguez, and P. Zoller, Phys. Rev. A **64**, 033609 (2001).
- [10] J. Kinnunen, M. Rodriguez, and P. Törmä, Phys. Rev. Lett. **92**, 230403 (2004).
- [11] J. Kinnunen, M. Rodriguez, and P. Törmä, Science **305**, 1131 (2004).
- [12] C. Chin and P. S. Julienne, Phys. Rev. A **71**, 012713 (2005).
- [13] Y. He, Q. Chen, and K. Levin, Phys. Rev. A **72**, 011602 (2005).
- [14] Y. Ohashi and A. Griffin, Phys. Rev. A **72**, 063606 (2005).
- [15] A. Perali, P. Pieri, and G. C. Strinati, Phys. Rev. Lett. **100**, 010402 (2008).
- [16] P. Massignan, G. M. Bruun, and H. T. C. Stoof (2008), arXiv:0709.3158.
- [17] S. Basu and E. J. Mueller (2007), arXiv:0712.1007.
- [18] M. Zwierlein, Z. Hadzibabic, S. Gupta, and W. Ketterle, Phys. Rev. Lett. **91**, 250404 (2003).
- [19] Z. Yu and G. Baym, Physical Review A **73**, 063601 (2006).
- [20] M. Punk and W. Zwerger, Phys. Rev. Lett. **99**, 170404 (2007).
- [21] G. Baym, C. J. Pethick, Z. Yu, and M. W. Zwierlein, Phys. Rev. Lett. **99**, 190407 (2007).
- [22] D. D. Osheroff, R. C. Richardson, and D. M. Lee, Phys. Rev. Lett. **28**, 885 (1972).
- [23] D. D. Osheroff, W. J. Gully, R. C. Richardson, and D. M. Lee, Phys. Rev. Lett. **29**, 920 (1972).
- [24] A. J. Leggett, Phys. Rev. Lett. **29**, 1227 (1972).
- [25] J.-P. Martikainen and P. Törmä, Phys. Rev. Lett. **95**, 170407 (2005).
- [26] J. Kinnunen and P. Törmä, Phys. Rev. Lett. **96**, 070402 (2006).
- [27] G. Vidal, Phys. Rev. Lett. **91**, 147902 (2003).
- [28] D. Jaksch, C. Bruder, J. Cirac, C. W. Gardiner, and P. Zoller, Phys. Rev. Lett. **81**, 3108 (1998).
- [29] G. Vidal, Phys. Rev. Lett. **93**, 040502 (2004).
- [30] J. J. Garcia-Ripoll, New. J. Phys. **8**, 305 (2006).